TU Delft

Delft University of Technology

Robust Signal Control of Exit Lanes for Left-Turn Intersections with the Consideration of Traffic Fluctuation

Chen, Kaijia; Zhao, Jing; Knoop, Victor L.; Gao, Xing

DOI
10.1109/ACCESS.2020.2977134

Publication date
2020

Document Version
Final published version

Published in
IEEE Access

Citation (APA)
Chen, K., Zhao, J., Knoop, V. L., & Gao, X. (2020). Robust Signal Control of Exit Lanes for Left-Turn Intersections with the Consideration of Traffic Fluctuation. *IEEE Access*, *8*, 42071-42081. Article 9018258. https://doi.org/10.1109/ACCESS.2020.2977134

Important note
To cite this publication, please use the final published version (if applicable).
Please check the document version above.

Copyright
Other than for strictly personal use, it is not permitted to download, forward or distribute the text or part of it, without the consent of the author(s) and/or copyright holder(s), unless the work is under an open content license such as Creative Commons.

Takedown policy
Please contact us and provide details if you believe this document breaches copyrights.
We will remove access to the work immediately and investigate your claim.

This work is downloaded from Delft University of Technology.
For technical reasons the number of authors shown on this cover page is limited to a maximum of 10.

IEEE Access
Multidisciplinary ⋮ Rapid Review ⋮ Open Access Journal

Received February 14, 2020, accepted February 24, 2020, date of publication February 28, 2020, date of current version March 11, 2020.

Digital Object Identifier 10.1109/ACCESS.2020.2977134

Robust Signal Control of Exit Lanes for Left-Turn Intersections With the Consideration of Traffic Fluctuation

KAIJIA CHEN[1], JING ZHAO[1,2], VICTOR L. KNOOP[2], AND XING GAO[1]
[1]Department of Traffic Engineering, University of Shanghai for Science and Technology, Shanghai 200093, China
[2]Transport and Planning, Delft University of Technology, 2628 Delft, The Netherlands

Corresponding author: Jing Zhao (jing_zhao_traffic@163.com)

This work was supported in part by the National Natural Science Foundation of China under Grant 71971140.

ABSTRACT Traffic throughput at intersections can be improved by using exit lanes for left-turning (EFL), tidal flow lanes near an intersection, which has been recently introduced. This paper considers the operational robustness of the EFL intersection in relation to the control scheme applied to the traffic light setting. For safety and efficiency, it is important that the tidal lanes are emptied before traffic in the opposing direction uses these lanes. Hence, the signal control should not only be optimized for the mean value but be robust for all kinds of fluctuations. This paper formulates a traffic control scheme using robust optimization, i.e. an optimization scheme which explicitly accounts for extreme events. The fluctuation of traffic is considered from three aspects: the distribution of traffic demand, the distribution of base saturation flow rate, and the distribution of actual travel speed. Via a case study and extensive numerical analysis, we find that the established robust optimization method produces an efficient design of signal control and design speed at the EFL intersection under traffic demand and supply fluctuations. Though the optimization method is now applied to intersections with an EFL, it is considered useful for all intersections with high fluctuation of traffic demand and saturation flow rate.

INDEX TERMS Exit-lanes for left-turn intersection, robust optimization, signal control, unconventional intersections.

I. INTRODUCTION

With rapid economic development and urbanization, roads in many cities have become increasingly congested. As the bottlenecks of the road network, improving the operational efficiency of intersections has been concerned by researchers for a long time. However, the effects of traditional methods, such as expanding geometric space and optimizing signal control, are getting more and more limited due to the rapid expansion of traffic demand. Faced with the problem of increasingly oversaturated intersections, various unconventional intersections have been proposed to further improve the capacity of intersections, including median U-turn intersections [1]–[5], continuous flow intersections [6]–[10], tandem intersections [11]–[14], uninterrupted flow intersections [15], [16], special width approach lanes intersections [17], exit-lanes for left-turn intersections [18], [19].

The associate editor coordinating the review of this manuscript and approving it for publication was Mauro Gaggero.

The exit-lanes for left-turn (EFL) intersection is one of the newly proposed unconventional intersections [18]. Its characteristic is that part of the exit lanes is set as a mixed-use area, which can be utilized as both exit lanes and left-turn lanes respectively at different stages of a signal cycle through the coordination control of main and pre-signal. Thus, the intersection capacity can be enhanced obviously with additional left-turn lanes. The EFL intersection has been taken into application in several cities in China, such as Jinan, Handan, Shenzhen, Wuhan, Chongqing, Nanchang, and Liaocheng. Some studies on the deterministic optimization design method for EFL intersections have been conducted.

The existing fixed signal timing models for EFL intersections assume that both the traffic demand and the saturation flow rate in each direction are given, which is generally the mean value during the survey period. However, actual traffic demand in practice fluctuate significantly [20]–[23]. The drivers' behavior has something different at EFL intersections due to their unfamiliarity to this innovative design.

This work is licensed under a Creative Commons Attribution 4.0 License. For more information, see http://creativecommons.org/licenses/by/4.0/

This will result in the fluctuation of saturation flow rate at EFL intersections [24]. Such fluctuations of traffic demand and supply have a significant impact on the actual operation at EFL intersections. On the other hand, improper disposals may also cause left-turn vehicles to be trapped in the mixed-use area, which seriously affecting operational efficiency. Thus, a robust control method, which can adapt to traffic fluctuations, should be established to keep the operational robustness of EFL intersections.

Although there have been several studies on robust optimization at conventional intersections, the previous robust optimization methods mainly consider the traffic demand fluctuation, which is independent of the design scheme. As for EFL intersections, in addition to the fluctuation of the traffic demand, it may also cause the fluctuation of the saturation flow rate due to the unfamiliarity of the driver. Moreover, the saturation flow rate will change with the design scheme [24]. For example, due to the travel speed fluctuations, designing different clearance time of the mixed-use area will result in different retention probability of left-turn vehicles in the mixed-use area, forming different saturation flow rate. Therefore, the problem of optimizing the signal control robustness for EFL intersections is more complicated than that of conventional intersections. Besides traffic demand fluctuations, the fluctuations of the saturation flow rate should also be considered.

This paper aims to propose a robust signal control model for EFL intersections under the condition of traffic fluctuations. The traffic fluctuations are considered from the following three aspects: (1) the distribution of traffic demand, (2) the distribution of base saturation flow rate, (3) the distribution of the actual travel speed. They are the external inputs of the proposed model. The rest of this paper is organized as follows. The literature review is presented in Section II. The operational characteristics of EFL intersections are introduced in Section III. Section IV presents the robust optimization model. Section V validates the accuracy of the algorithm and the effect of robust optimization. More detailed analyses of the effectiveness of the proposed model are performed by extensive numerical experiments in Section VI. Conclusions are drawn at the end of the paper.

II. LITERATURE REVIEW

The relevant studies of the paper mainly contain three aspects: the operational efficiency of the EFL intersection, the safety of the EFL intersection, and the robust optimization at intersections.

For operational efficiency, Zhao *et al.* [18] established an overall optimization framework including lane assignment, length of the mixed-use area and signal control parameters. Based on this design idea, Wu *et al.* [19] optimized the position of the median opening and the signal timing of pre-signal based on the capacity and delay analysis of the left-turn movement. Su *et al.* [25] studied the operational advantage of such design. By adding more consideration to the unique queuing behavior at the pre-signal, Liu *et al.* [26] proposed an improved shockwave-based method to estimate the maximum left-turn queue length. Zhao *et al.* [24] proposed a saturation flow rate adjustment model for EFL control based on field data. An actuated signal control strategy was further developed to improve the operations of EFL intersections [27].

For operational safety, the driver's reaction to such design under various traffic signs and markings was first analyzed using a high fidelity driving simulator [28]. Results indicate that although the confusion and hesitation of drivers are ubiquitous when encountering an EFL intersection for the first time, such design is not likely to pose a serious safety risk. Moreover, the data collected in the real-world were used to evaluate the safety of the EFL intersections [29]. The results show that the potential safety problems of EFL intersections include higher percentages of red-light violations at pre-signals, wrong-way violations during peak hours, and lower travel speeds in mixed-usage-areas. However, these risks can be relieved by providing more guiding information and strengthening the law-enforcement, e.g. installing cameras to investigate violation maneuvers.

In the existing signal control methods, there are many approaches to address the fluctuations in traffic, including the robust signal control, actuated control, and adaptive control [30]–[33]. In this paper, the robust signal control method is used. For the robust optimization at intersections, many studies have been conducted under the condition of traffic demand fluctuations at conventional intersections to obtain a control scheme that is most suitable for traffic volume fluctuations. Heydecker [20] studied the effect of traffic fluctuations on signal timing and formed a set of appropriate control schemes aiming at the minimum mean delay by investigation data. Ribeiro [34] proposed a new control scheme with good universality, and the results of the TRANSYT test showed that this scheme still performed well in the case of traffic flow fluctuations. Considering the traffic demand fluctuations, Park and Kamarajugadda [35] proposed a dynamic signal control method based on the genetic algorithm, and the simulation results of CORSIM indicated that this method had better robust performance than that of the SYNCHRO control scheme. Based on the scenarios, Yin [23] put forward three kinds of robust optimization schemes that could be well adapted to traffic fluctuations. Based on the robust optimization model, Li [36] improved the solution algorithm and proposed a discrete modeling method to obtain the global optimum solution by converting the problem into a binary integer program. Tong *et al.* [37] proposed a stochastic programming model to optimize the adaptive signal control. With the comparison with the deterministic linear programming model, it shows that the proposed stochastic programming model can reduce total vehicle delay and queue length, and improve throughput. Yu *et al.* [38] proposed a robust optimization model for the integrated design of lane allocation and signal timing for isolated intersections. Hao *et al.* [39] proposed a robust optimization model of signal timing for unsaturated intersections. The minimum of the

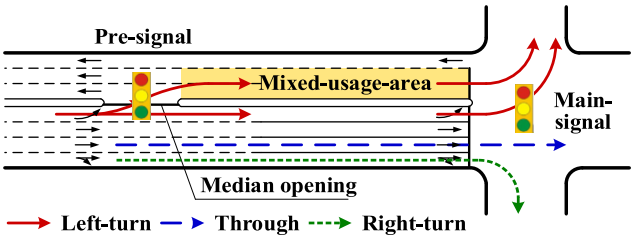

FIGURE 1. Geometric design of EFL intersection.

combination of the average delay and the mean square error of average delay is considered as objective. The robust optimization methods were also widely analyzed in coordination control [40], [41], bus priority control [42]–[44], network design [45]–[49], and multi-objective optimization [50], [51].

According to the literature review, one can find that the previous robust optimization methods mainly consider the traffic demand fluctuation. Therefore, it is still a challenge to establish a robust signal control model for EFL intersections under the condition of traffic demand and supply fluctuations.

III. INTRODUCTION OF EFL INTERSECTION

The geometric structure of the EFL intersection is shown in Fig. 1 [18], where the yellow zone is the mixed-use area. The mixed-use area can be used as exit lanes or left-turn lanes, respectively, during different stages of a signal cycle. The median opening is set at the upstream of the main stop line, equipped with pre-signal to control vehicles. The mixed-use area is used as exit lanes when the pre-signal is red, whereas it is left-turn lanes when the pre-signal is green. When the left-turn green light at the main signal is turned on, both vehicles in the mixed-use area and conventional left-turn vehicles can turn left at the same time to pass through the intersection. Compared to conventional intersections, several left-turn lanes are added at EFL intersections. That is why the capacity of whole intersection is enhanced dramatically. Please note, the layout of the intersection is the input of the proposed model. There are some constraints on the layout design of the EFL intersection, including that (1) the shared left-turn and through lane should be forbidden; (2) at least one normal approach lane should be assigned for the left-turn; (3) the total number of left lanes should not be greater than the number of exit lanes in the receiving leg [18].

As for signal control, pre-signals are added at EFL intersections. Moreover, the clearance time needs to be long enough to guarantee the smooth emptying of vehicles in the mixed-use area. It means the green light at the pre-signal shall be turned on after the end time of previous conflict phase and turned off before the end of left-turn green light at the main signal. The phase plan at EFL intersections is shown in Fig. 2. The main signal is dual- ring control, and the pre-signal corresponds to the main signal one-by-one according to a specific phase sequence.

In this paper, we will propose a signal timing model for EFL intersections with the consideration of traffic

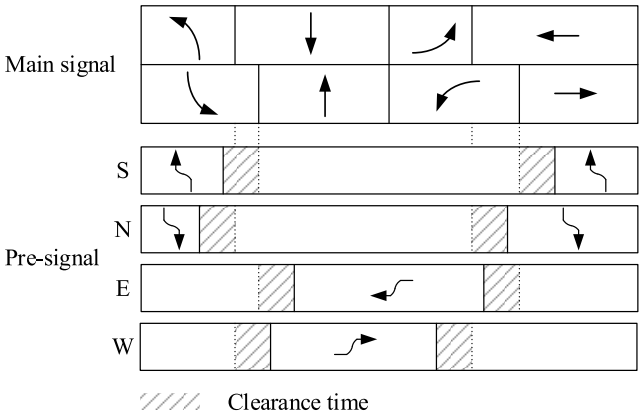

FIGURE 2. Phase plan of EFL intersection.

fluctuations from the following three aspects: (1) the distribution of traffic demand, (2) the distribution of base saturation flow rate, (3) the distribution of the actual travel speed.

IV. OPTIMIZATION MODEL

To enhance the robustness of operational efficiency at EFL intersections, a scenario-based robust optimization method was adopted in this paper [52]. The principle of this method is to put forward a set of traffic scenarios $\mathcal{S}$ to express the fluctuation of traffic demand, saturation flow rate, and actual travel speed as a finite number of discrete traffic scenario $k \in \mathcal{S}$ and the occurrence probability π^k. For traffic scenario k, the traffic demand q^k, the saturation flow rate s^k, and the actual travel speed v^k are given. Any design scheme a will run in all scenarios. Then, the evaluation result d_a^k can be obtained in scenario k. After all scenarios are performed, the evaluation result set $\mathcal{D}_a$ for design scheme a can be obtained. Then, the optimal design scheme a^* for scenario set $\mathcal{S}$ can be obtained by the optimization algorithm. The decision variables in this study include cycle length C, green time of each phase G and design speed v_s.

To facilitate the model presentation, the notations used hereafter are summarized in Table 1.

A. OBJECTIVE FUNCTION

Delay is adopted as the evaluation indicator in this study because it can well represent the operation efficiency of an independent intersection. With the consideration of traffic fluctuations, the operational efficiency and robustness of a design scheme can be reflected by the mean and standard deviation of the evaluation results under all scenarios, respectively. The standard deviation is a measure of the variation. A low standard deviation indicates that the values tend to be close to the mean, while a high standard deviation indicates that the values are spread out over a wider range. Since the overall efficiency and robustness conflict with each other, a tradeoff is needed. The mean-standard deviation model (abbreviated as MSD model) is used to describe the tradeoff,

TABLE 1. Notations of key model parameters and variables.

Notations	Meaning
$\mathcal{S}$	Scenario set
k	The indices of scenarios
$\mathcal{L}$	Set of legs
i	The indices of legs, $i \in \mathcal{L}$, $i = 1,2,3,4$ respectively represent east, south, west, and north leg
$\mathcal{J}$	Set of movements
j	The indices of movements, $j \in \mathcal{J}$, $j = 1,2,3$ respectively represent left-turn, through movement and right-turn
π^k	Occurrence probability of scenario k
γ	Weighting coefficient, $0 \le \gamma \le 1$, and the value of γ depends on whether the decision-maker prefers efficiency or robustness
d	Vehicular delay of the intersection, s/veh
d_{ij}	Vehicular delay of movement j from leg i, s/veh
d_a^k	Vehicular delay of scheme a in scenario k, s
c_{ij}	Capacity of movement j from leg i, veh/h
T	Duration of the analysis period, h
l_i	Length of the mixed-use area on leg i, m.
β	Number of exit lanes
q_{ij}	Traffic demand of movement j from leg i, veh/h
v	Actual travel speed of left-turn vehicles in the mixed-use area at the end of green time, m/s
v_s	Design speed for calculating the clearance time, m/s
s_{ij}	Saturation flow rate, veh/h
f	Correction coefficient of the influence of left-turn vehicles stranded in the mixed-use area on the through saturation flow rate at the main signal
f^p	Correction coefficient of the influence of vehicles stranded in the mixed-use area on the left-turn saturation flow rate at the pre-signal
C	Cycle length, s
$C_{\min}$	Minimum cycle length, s
$C_{\max}$	Maximum cycle length, s
g_{ij}	Start of green of movement j from leg i, s
G_{ij}	Duration of green of movement j from leg i, s
g_i^p	Start of green of the pre-signal on leg i, s
G_i^p	Duration of green of the pre-signal on leg i, s
$G_{ij\min}$	Minimum green time of movement j from leg i, s
I	Green interval, s

which can be specialized by Eq. (1).

$$\min_{C,G,v_s} \gamma \cdot \sum_{k\in\mathcal{S}} \pi^k d_a^k (C,G,v_s) + (1-\gamma) \cdot \sqrt{\sum_{k\in\mathcal{S}} \pi^k \left(d_a^k (C,G,v_s) - \sum_{k\in\mathcal{S}} \pi^k d_a^k (C,G,v_s) \right)^2} \quad (1)$$

The proposed model (a robust optimization method) is essentially different from the traditional deterministic model. The difference lies in whether the fluctuations of the input parameters are considered. The traditional deterministic model takes the mean values of traffic demand and saturation flow rate as inputs. It means the result will not change when the mean values of input parameters maintain the same but the distributions are different. In the proposed model, the optimization result will change when the distributions of input parameters change.

B. CONSTRAINTS

1) CALCULATION OF THE VEHICULAR DELAY

The calculation framework of HCM [53] delay was adopted in this paper to estimate the delay per vehicle, as shown in Eqs. (2) and (3). However, the vehicle retention problem in the mixed-usage area is an operational risk of the EFL intersection. If the vehicles in the mixed-usage area cannot be cleared before the end of a phase, the saturation flow rate of the subsequent movement will be reduced significantly. It happens at both the main signal and pre-signal. Therefore, the capacity should be adjusted, as shown in Eq. (4).

At the main signal, the clearance time is calculated based on the length of the mixed-usage-area and the design speed. Once the length of the mixed-usage-area is given, the clearance time can be determined by the design speed. When the clearance time between the end of left-turn green at the main signal and the end of green at the pre-signal is less than the actual time for vehicles to pass through the mixed-use area, left-turn vehicles will be stranded. In the deterministic signal control optimization, this problem can be solved easily by setting corresponding constraints to ensure that the clearance time is longer than the travel time of the mixed-use area. However, in practice, it is difficult to fully satisfy all the above constraints on account of travel speed fluctuations. However, if the signal timing is set too conservatively, the green time will be reduced, while if the signal timing is aggressive, it may lead to the retention of vehicles and reduce the number of available through lanes during the next phase. Both of these situations affect the saturation flow. Therefore, the correction equation of the saturation flow rate at main signal is shown in Eq. (5). It means that the saturation flow rate will be adjusted according to the ratio of the number of the blocked lanes and the total number of exit lanes.

At the pre-signal, the clearance time is also determined by the design speed. When the clearance time, between the start of green at the pre-signal and the end of green of the left-turn from the right adjacent leg, is less than the actual time for vehicles to pass through the mixed-use area, the left-turn vehicles from the right adjacent leg will be stranded. For the sake of traffic safety, left-turn vehicles have to wait for the clearance of the mixed-use area before they enter the mixed-use area at the pre-signal. The green time at the pre-signal will be reduced in this case. Similarly, the correction equation of saturation flow rate at pre-signal is shown in Eq. (6). It means that the saturation flow rate will be adjusted according to the ratio of the blocked time and the green time.

$$d = \frac{\sum_i \sum_j d_{ij} q_{ij}}{\sum_i \sum_j q_{ij}} \quad (2)$$

$$d_{ij} = \frac{0.5C\left(1-\frac{G_{ij}}{C}\right)^2}{1-\left(\min\left(1,\frac{q_{ij}}{c_{ij}}\right)\frac{G_{ij}}{C}\right)} + 900T\left[\left(\frac{q_{ij}}{c_{ij}}-1\right) + \sqrt{\left(\frac{q_{ij}}{c_{ij}}-1\right)^2 + \frac{4q_{ij}}{c_{ij}^2 T}}\right] \quad (3)$$

$$c_{ij} = s_{ij}\frac{g_{ij}}{C}ff^p \tag{4}$$

$$f = \begin{cases} \dfrac{\beta - 1}{\beta}, & v < v_s \\ 1, & v \geq v_s \end{cases} \tag{5}$$

$$f^p = 1 - \frac{max\left(\frac{l_i}{v} - \frac{l_i}{v_s}, 0\right)}{G_i^p} \tag{6}$$

2) CONSTRAINTS OF THE MAIN SIGNAL

According to the signal phase plan shown in Fig. 2, the start and the duration of green of each movement should meet following requirements, as listed in Eqs. (7)-(11). Without loss of generality, the start of green of left-turn from the south and north legs is set to be 0, as shown in Eq. (7). The start of green of the through movement from a leg equals the end of the left-turn phase from the opposing leg, as shown in Eqs. (8) and (9). The start of green of the left-turn from east and west legs should be the same, which equals the end of through phase from the north and south legs, as shown in Eqs. (10) and (11). The end of through phase from the east and west legs is equal to the cycle length, as shown in Eq. (12). Moreover, the cycle length should be within a reasonable range and the duration of green of each movement must be no less than the minimum green time, as shown in Eqs. (13) and (14), respectively.

$$g_{i1} = 0, \quad \forall i \in \{2, 4\} \tag{7}$$

$$g_{i2} = g_{(i+2)1} + G_{(i+2)1} + I, \quad \forall i \in \{1, 2\} \tag{8}$$

$$g_{i2} = g_{(i-2)1} + G_{(i-2)1} + I, \quad \forall i \in \{3, 4\} \tag{9}$$

$$g_{11} = g_{31} \tag{10}$$

$$g_{i1} = g_{(i+1)2} + G_{(i+1)2} + I, \quad \forall i \in \{1, 3\} \tag{11}$$

$$g_{i2} + G_{i2} + I = C, \quad \forall i \in \{1, 3\} \tag{12}$$

$$C_{\min} \leq C \leq C_{\max} \tag{13}$$

$$G_{ij} \geq G_{ij\min}, \quad \forall i \in \mathcal{L},\ j \in \mathcal{J} \tag{14}$$

3) CONSTRAINTS OF PRE-SIGNAL

According to Fig. 2, the pre-signal needs to be coordinated with the main signal. To guarantee the smooth clearance of vehicles in the mixed-use area, the start of the green of pre-signal should be equal to the end of the left-turn phase at the right adjacent leg plus the clearance time required for the vehicles to pass through the mixed-use area, as shown in Eq. (15). Similarly, the end of green of pre-signal should be equal to the end of left-turn green time at the main signal on the same leg minus the clearance time required for the vehicles to pass through the mixed-use area, as shown in Eq. (16).

$$g_i^p = g_{(i-1)1} + G_{(i-1)1} + I + \frac{l_i}{v_s}, \quad \forall i \in \mathcal{L} \tag{15}$$

$$g_i^p + G_i^p = g_{i1} + G_{i1} - \frac{l_i}{v_s}, \quad \forall i \in \mathcal{L} \tag{16}$$

C. SOLUTION

Since the objective function is non-convex and non-differentiable [23], [54], [55] and the model contains nonlinear constraints, it is difficult to solve by traditional optimization algorithms. A heuristic algorithm is often used to solve this problem [38], [56], [57]. Therefore, this model was figured out based on the genetic algorithm (GA) in this paper, and the procedure is shown below. For the nonlinearity of the constraints, the control variable v_s makes the constraints (5) and (6) nonlinear. Even if these constraints can be linearized, there is not much difference for the solver. The nonlinear, non-convex and non-differentiable of the objective function is the main reason to choose the genetic algorithm (GA) to solve the problem.

Step 1: Parameter input. Parameters include the intersection geometric structure, the distribution of traffic demand, the distribution of base saturation flow rate, and the distribution of actual travel speed. Go to step 2.

Step 2: Generation of traffic scenarios. Traffic scenario set S will be randomly generated according to the distributions in step 1. Go to step 3.

Step 3: Generation of signal control schemes based on genetic algorithm. Schemes include initial population (the population is 40), selection (by pure random selection), crossover (by simulating binary-valued crossover, the probability of crossover is 0.9), mutation (by inconsistent mutation, the probability of mutation is 0.1), recombination of parent and offspring populations during iteration. Go to step 4.

Step 4: Calculation of fitness. The individual schemes will be performed in each traffic scenario, and then their individual fitness will be calculated according to the objective function (Eq. (1)). The first 50% of optimal individuals will be selected to survive. Go to step 5.

Step 5: Judgment of termination criteria. The iterative process will be stopped when the improvement in the fitness in the sequential 10 iterations are all less than ξ (10^{-4}); otherwise, it will be transferred to step 3.

V. CASE STUDY

We applied the proposed model to a case study and compared it with a standard control scheme (with EFL). The introduction of the case study intersection, control schemes, and comparison results will be described.

A. INPUT DATA

The accuracy of the algorithm and the effect of robust optimization were tested by a case study. The intersection of Lianfang Road and Fuhebei Street in Handan was selected in this paper, as shown in Fig. 3. The EFL control was used in all legs. The geometric layout is shown in Table 2. The statistical survey results during peak hours are listed in Table 3, including traffic demand, base saturation flow rate, and actual travel speed of vehicles passing through the mixed-use area. The minimum and maximum cycle length are set to be 90 s and 150 s, respectively. The shortest green time is 5 s. The green interval is 5 s. The duration of the analysis period is 1 h.

(a) West and North legs

(b) East and South legs

FIGURE 3. Case study intersection.

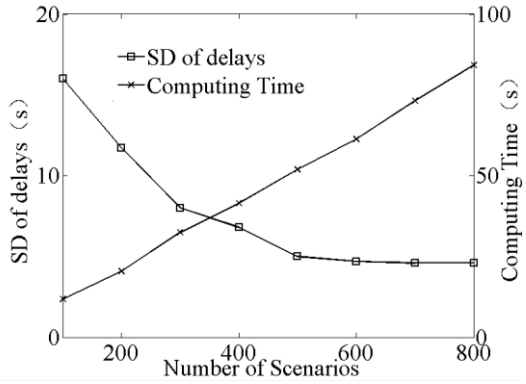

FIGURE 4. Effect of the scenario number.

According to the distribution in Table 3, scenarios in line with the actual traffic conditions can be generated. Two things need to clarify firstly before optimizing this intersection.

The first one is the number of scenarios in the scenario set. More scenarios are conventionally conducive to draw up a better scheme, whereas too many scenarios will greatly increase the calculation time in turn. Mulvey *et al.* [52] found that there is no need to list too many scenarios to get close to the ideal solution after detailed study. On this basis, we analyzed the trend of optimization effect and computing cost with the change of scenario number. As shown in Fig. 4, the cost is directly proportional to the scenario number. When the number exceeds 500, the optimization effect turns stable. Thus 500 is selected as a scenario number in this paper for optimal design. In this case, the model can be solved in one minute. Since the proposed robust signal control method is designed for fixed-time control, which will not be updated frequently in the real world, the computing time is acceptable. To further improve the computational efficiency, the distributed computing method can be used.

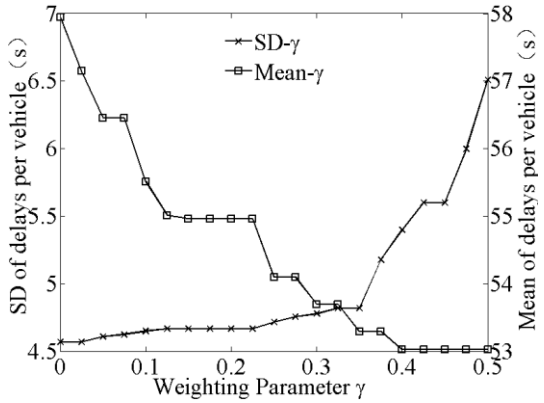

FIGURE 5. Tradeoff of efficiency-robustness with the change of γ.

TABLE 2. Layout of the case study intersection.

Leg		North	South	West	East
Length of mixed-use area (m)		50	50	60	60
Number of lanes	Exit lanes	3	3	3	3
	Mixed-use area	1	1	2	2
	Exclusive left-turn lanes	1	1	1	1
	Exclusive through lanes	3	3	3	3
	Shared through and right-turn lanes	0	1	1	1
	Exclusive right-turn lane	1	0	0	0

The second one is the value of the weighting coefficient γ in the proposed model. The effect of weighting coefficient γ was discussed since it determines the attitude towards robustness and efficiency. According to Fig. 5, the standard deviation of delay increases whereas the mean delay decreases as γ increases. In this case, the standard deviation of delay increases rapidly whereas the decrease of mean delay tends to be stable when γ is higher than 0.35. Therefore, γ was set to be 0.35 in the following analysis to consider the full extent of robustness while maintaining efficiency.

B. OPTIMIZATION CONTROL SCHEMES

The optimization control schemes of the traditional deterministic control method and the proposed robust optimization method are listed in Table 4. The traditional control scheme is established based on the mean value of traffic volume, saturation flow rate, and actual travel speed as input data. For the proposed model, γ was 0.35 and 1 respectively according to the above analysis, where $\gamma = 1$ represents that only efficiency (minimum mean delay) is considered.

To verify the accuracy of the algorithm, Fig. 6 shows the value of the optimization objective of the proposed model under different design speeds and cycle lengths. If the algorithm is valid, the results of the proposed model should be exactly the minimum points of curves. The results of Fig. 6 have proved that the proposed algorithm can find the minimal value of the objective and obtain the optimal solution for the proposed model.

TABLE 3. Statistical results of traffic fluctuations.

Movement	Traffic flow			
	Mean	SD	Min	Max
N-L	730	100	230	930
N-T	577	45	490	665
N-R	145	20	90	165
S-L	759	70	620	900
S-T	509	40	430	590
S-R	105	18	70	141
W-L	541	65	410	670
W-T	581	46	500	680
W-R	120	22	80	165
E-L	516	60	400	630
E-T	620	42	560	695
E-R	134	21	90	175
Movement	Saturation flow rate			
	Mean	SD	Min	Max
N-L	1620	120	1380	1860
N-T	1620	120	1380	1860
N-R	1600	100	1370	1800
N-P	1425	135	1160	1690
S-L	1500	128	1250	1750
S-T	1490	128	1240	1740
S-R	1490	128	1240	1740
S-P	1480	133	1220	1740
W-L	1500	126	1250	1750
W-T	1500	126	1250	1750
W-R	1500	126	1250	1750
W-P	1487	151	1190	1780
E-L	1540	123	1300	1780
E-T	1540	123	1300	1780
E-R	1540	123	1300	1780
E-P	1460	105	1360	1770
Movement	Actual travel speed			
	Mean	SD	Min	Max
All	7.5	1.48	4.2	13

Note: N, S, W and E respectively represent north, south, west, east leg; L, T, R, and P respectively represent left-turn, through movement, right-turn and the entering movement at pre-signal; SD is the standard deviation; Min and Max respectively represent the minimum and maximum value.

TABLE 4. Optimized control schemes.

Control variable	Traditional (s)	MSD-1.0 (s)	MSD-0.35 (s)
G_{21}	21	21	23
G_{42}	17	17	20
G_{31}	20	20	22
G_{12}	12	13	15
G_{41}	21	20	22
G_{22}	17	18	21
G_{11}	20	20	22
G_{32}	12	13	15
G_1^p	16	16	17
G_2^p	16	17	18
G_3^p	17	18	19
G_4^p	17	17	18
C	90	91	100
v_s	6	5.85	4.9

C. COMPARISON ANALYSIS

To verify and compare the effectiveness of robust optimization schemes, they are evaluated by Monte Carlo simulation. 2000 traffic scenarios were generated according to the distribution of Table 3 to make the evaluation results more accurate. The results are shown in Table 5. Using the traditional scheme as the benchmark, the effect of robust optimization model was analyzed.

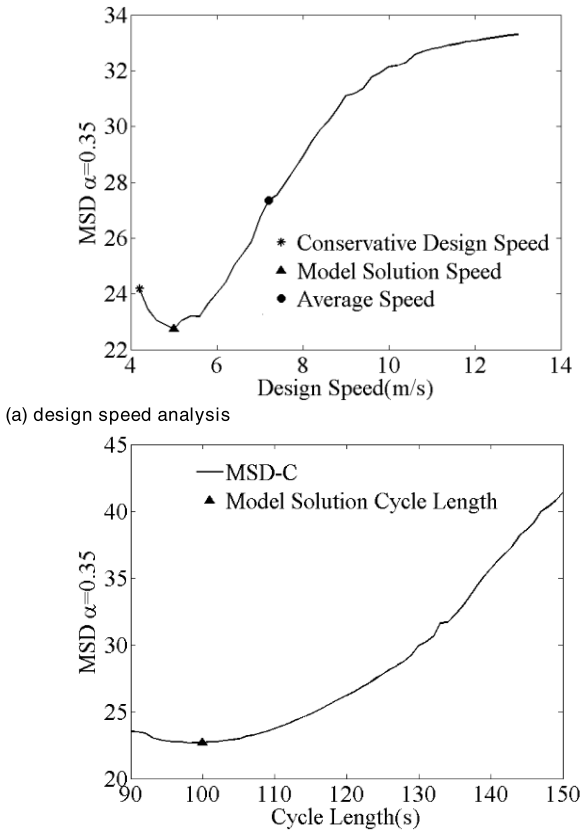

FIGURE 6. Algorithm accuracy test.

Overall, the performance of the traditional scheme, which is obtained based on the mean value of traffic volume, base saturation flow rate, and actual travel speed, is acceptable for the indicator of the mean delay. It is consistent with the conclusion reached by Heydecker [20] and Yin [23] when optimizing the conventional intersection. However, the optimal mean delay cannot be reached by the traditional scheme, whereas it should be obtained by MSD-1.0 mode, as shown in Table 5.

Compared with the traditional scheme, the MSD-0.35 model can highly enhance the robustness of operation (more than 40% decrease in standard deviation of delay, and more than 10% decrease in worst-case delay), whereas maintaining the original mean delay per vehicle (less than 3% increase). Therefore, the robust optimization model generally performs better when obtaining the robust optimal signal timing for EFL intersections. It can greatly improve robustness without efficiency loss.

VI. SENSITIVITY ANALYSIS

To further analyze the adaptability of the proposed robust optimization method, sensitivity analysis of critical parameters was carried out to explore the influence of traffic demand and supply fluctuations on optimization benefits.

TABLE 5. Comparisons of control schemes.

Indicator		Traditional	MSD-0.35	MSD-1.0
Mean delay		52.5	54	51.7*
SD of delay		9.3	5.0*	8.0
Max delay		132.6	116*	121.9
Change (%)	Mean delay	-	2.86	-1.52
	SD of delay	-	-46.24	-13.98
	Max delay	-	-12.51	-8.07

Note: SD denotes the standard deviation, and Max denotes the maximum value.

TABLE 6. Layout of the intersection for sensitivity analysis.

Leg		North	South	West	East
Length of mixed-use area (m)		50	50	50	50
Number of lanes	Exit lanes	3	3	3	3
	Mixed-use area	1	1	1	1
	Exclusive left-turn lanes	1	1	1	1
	Exclusive through lanes	2	2	2	2
	Shared through and right-turn lanes	0	0	0	0
	Exclusive right-turn lane	1	1	1	1

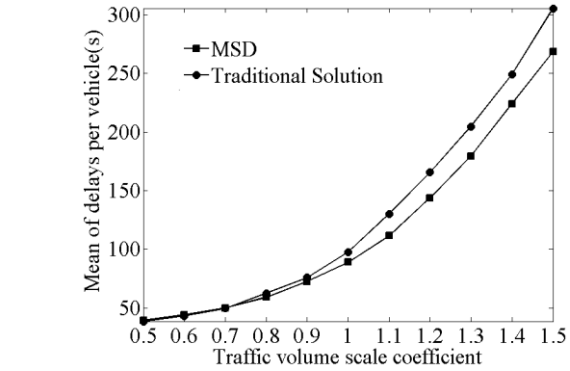

(a) Mean vehicular delay

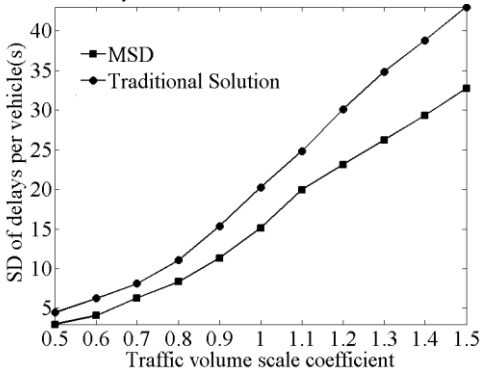

(b) Standard deviation of delay

FIGURE 7. Influence of traffic demand.

A. INPUT DATA

The geometric layout of the intersection used for sensitivity analysis is shown in Table 6. The distribution of traffic demand, base saturation flow rate, and actual travel speed are listed in Table 7. Other parameters are the same as in Section IV.A.

B. INFIUENCE OF TRAFFIC DEMAND

Scale the mean traffic volume of each movement with the scaling range from 0.5 to 1.5. The results are shown in Fig. 7.

TABLE 7. Distribution of traffic for sensitivity analysis.

Movement	Traffic flow			
	Mean	SD	Min	Max
N-L	700	100	500	900
N-T	650	75	500	800
N-R	150	22	105	190
S-L	500	70	360	640
S-T	700	90	520	880
S-R	125	16	95	158
W-L	550	65	420	680
W-T	600	70	460	740
W-R	140	20	103	185
E-L	650	70	510	790
E-T	500	60	380	620
E-R	95	15	70	125
Movement	Saturation flow rate			
	Mean	SD	Min	Max
N-L	1650	130	1390	1910
N-T	1620	120	1380	1860
N-R	1525	135	1260	1790
N-P	1400	135	1130	1670
S-L	1600	120	1360	1840
S-T	1500	110	1280	1720
S-R	1620	130	1360	1850
S-P	1450	120	1210	1690
W-L	1580	125	1330	1830
W-T	1550	120	1310	1790
W-R	1560	122	1320	1800
W-P	1450	150	1150	1750
E-L	1650	120	1410	1890
E-T	1600	125	1350	1850
E-R	1500	108	1270	1700
E-P	1550	125	1300	1800
Movement	Actual travel speed			
	Mean	SD	Min	Max
All	7.5	1.48	4.2	13

Note: N, S, W and E respectively represent north, south, west, east leg; L, T, R, and P respectively represent left-turn, through movement, right-turn, and the entering movement at pre-signal; SD is the standard deviation; Min and Max respectively represent the minimum and maximum value.

Generally, the increase in traffic volume will weaken the overall operational efficiency and robustness of each scheme. The mean delay increases linearly with the increasing traffic volume. It is in line with previous research conclusions on the relationship between delay and traffic volume [53].

With the increase of traffic volume, the difference of standard deviation of delay between the traditional scheme and robust optimization scheme increases gradually. It implies that traditional scheme becomes more and more unstable in operational efficiency with high traffic demand. On the contrary, the robust optimization scheme (MSD-0.35) performs much better and effectively improves the operational robustness. Therefore, although the proposed model is suitable for both under-saturated and over-saturated conditions, the benefit of the proposed method is more significant in high saturated cases.

C. INFIUENCE OF TRAFFIC DEMAND FLUCTUATION

Scale the standard deviation of traffic volume in each movement with the scaling range from 0.5 to 1.5. The results are shown in Fig. 8. Generally, the increase of traffic demand fluctuation will weaken the overall operational efficiency and

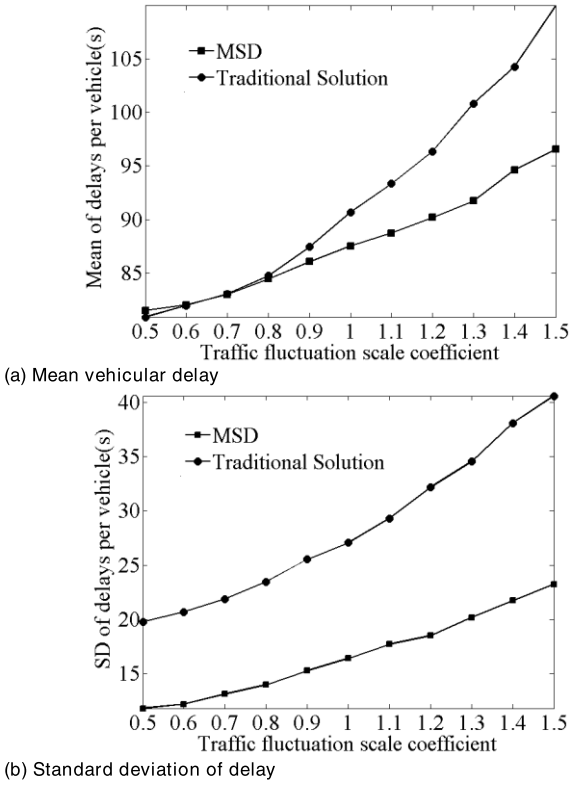

FIGURE 8. Influence of traffic demand fluctuation.

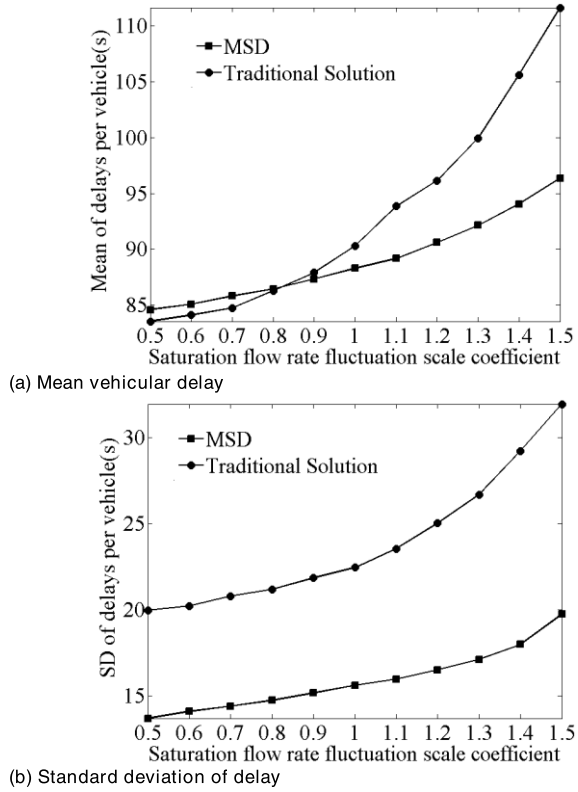

FIGURE 9. Influence of saturation flow rate fluctuation.

robustness of each scheme, especially the standard deviation of delay and worst-case delay.

As shown in Fig. 8(a), the traditional method outperforms the robust optimization method in mean delay under the condition that the fluctuation of the traffic demand is low. However, the mean delay of the traditional method increases rapidly with the increase of the traffic demand fluctuation. In the analysis, the proposed method (MSD-0.35) outperforms the traditional scheme in mean delay when the standard deviation researches 80% of the base settings shown in Table 7. It is because that the mean value of the traffic demand can no longer well represent the existing traffic scenarios when traffic demand fluctuation increases. Therefore, the robust optimization method can improve not only the robustness but also efficiency under high traffic demand fluctuation cases.

D. INFIUENCE OF SATURATION FLOW RATE FLUCTUATION

Scale the standard deviation of the saturation flow rate in each movement with the scaling range from 0.5 to 1.5. The results are shown in Fig. 8. Generally, the performance measures increase rapidly in the traditional method, which indicates that robust optimization methods have a better anti-interference ability.

Overall, when the saturation flow rate fluctuates slightly, the traditional scheme rivals the robust optimization scheme (MSD-0.35) in the mean delay. However, when the degree of fluctuation in saturation flow rate increases (researches 80% of the given value in Table 7), the robust optimization scheme (MSD-0.35) outperforms in the mean delay. It is because the mean value of the saturation flow rate can no longer well represent the existing traffic scenarios when the saturation flow rate fluctuation increases. Therefore, the proposed robust optimization model can dramatically enhance the efficiency and robustness of intersections under different degrees of the saturation flow rate fluctuation.

VII. CONCLUSION

For EFL intersections with fluctuating traffic demand and supply, the robustness of operational efficiency is essential. Therefore, considering the distribution of traffic demand, base saturation flow rate, and actual travel speed, a robust optimization model is established in this paper to minimize the mean-standard deviation. Through a case study and extensive numerical analysis, the accuracy of the algorithm, the value of the weighting coefficient in the mean-standard deviation model, and optimization benefits are analyzed. The following conclusions can be obtained.

(1) The proposed robust optimization model can optimize the design of the main signal, pre-signal, and design speed simultaneously. It has a promising application when traffic demand and saturation flow rate fluctuate wildly.

(2) The performance of the traditional scheme, which is obtained based on the mean value of traffic volume, base saturation flow rate, and actual travel speed, is acceptable for the indicator of the mean delay when the traffic fluctuation is slight.

(3) The proposed model can well balance the tradeoff between efficiency and robustness. The model can greatly enhance the operational robustness of effect (about 40% decrease in standard deviation of delay) on the basis of maintaining the original mean delay (less than 3% increase).

In this study, signal timings at main-signal and pre-signal are optimized. However, the operational efficiency can be further improved by optimizing the layout and signal timing simultaneously based on the lane-based method [54], [55], [58]. It is the direction of our future study. In practice, the study is a part of the control system. The stability of the control system can be discussed in future studies to improve the practical application effect.

REFERENCES

[1] P. Liu, J. J. Lu, H. Zhou, and G. Sokolow, "Operational effects of U-Turns as alternatives to direct left-turns," *J. Transp. Eng.*, vol. 133, no. 5, pp. 327–334, May 2007.

[2] M. El Esawey and T. Sayed, "Operational performance analysis of the unconventional median U-turn intersection design," *Can. J. Civil Eng.*, vol. 38, no. 11, pp. 1249–1261, Nov. 2011.

[3] S. S. Mohapatra and P. P. Dey, "Estimation of U-turn capacity at median openings," *J. Transp. Eng. A, Syst.*, vol. 144, no. 9, Sep. 2018, Art. no. 04018049.

[4] J. Zhao, W. Ma, K. L. Head, and Y. Han, "Improving the operational performance of two-quadrant parclo interchanges with median U-turn concept," *Transportmetrica B, Transp. Dyn.*, vol. 6, no. 3, pp. 190–210, Nov. 2016.

[5] P. Liu, J. J. Lu, and H. Chen, "Safety effects of the separation distances between driveway exits and downstream U-turn locations," *Accident Anal. Prevention*, vol. 40, no. 2, pp. 760–767, Mar. 2008.

[6] W. Hughes, R. Jagannathan, D. Sengupta, and J. E. Hummer, "Alternative intersections/interchanges: Information report (AIIR)," Federal Highway Admin., Washington, DC, USA, Tech. Rep. HRT-09-060, 2010, p. 340, vol. 1.

[7] X. Yang and Y. Cheng, "Development of signal optimization models for asymmetric two-leg continuous flow intersections," *Transp. Res. C, Emerg. Technol.*, vol. 74, pp. 306–326, Jan. 2017.

[8] R. Goldblatt, F. Mier, and J. Friedman, "Continuous flow intersections," *ITE J.*, vol. 64, pp. 35–42, Jul. 1994.

[9] J. Zhao, X. Gao, and V. L. Knoop, "An innovative design for left turn bicycles at continuous flow intersections," *Transportmetrica B, Transp. Dyn.*, vol. 7, no. 1, pp. 1305–1322, May 2019.

[10] X. Yang, G.-L. Chang, S. Rahwanji, and Y. Lu, "Development of planning-stage models for analyzing continuous flow intersections," *J. Transp. Eng.*, vol. 139, no. 11, pp. 1124–1132, Nov. 2013.

[11] Y. Xuan, C. F. Daganzo, and M. J. Cassidy, "Increasing the capacity of signalized intersections with separate left turn phases," *Transp. Res. B, Methodol.*, vol. 45, no. 5, pp. 769–781, Jun. 2011.

[12] W. Ma, H. Xie, Y. Liu, L. Head, and Z. Luo, "Coordinated optimization of signal timings for intersection approach with presignals," *Transp. Res. Rec.*, vol. 2355, no. 1, pp. 93–104, Jan. 2013.

[13] C. Yan, H. Jiang, and S. Xie, "Capacity optimization of an isolated intersection under the phase swap sorting strategy," *Transp. Res. B, Methodol.*, vol. 60, pp. 85–106, Feb. 2014.

[14] J. Zhao, J. Yan, and J. Wang, "Analysis of alternative treatments for left turn bicycles at tandem intersections," *Transp. Res. A, Policy Pract.*, vol. 126, pp. 314–328, Aug. 2019.

[15] Y. Liu and Z. Luo, "A bi-level model for planning signalized and uninterrupted flow intersections in an evacuation network," *Comput.-Aided Civil Infrastruct. Eng.*, vol. 27, no. 10, pp. 731–747, Aug. 2012.

[16] C. Xie and M. A. Turnquist, "Lane-based evacuation network optimization: An integrated lagrangian relaxation and tabu search approach," *Transp. Res. C, Emerg. Technol.*, vol. 19, no. 1, pp. 40–63, Feb. 2011.

[17] J. Zhao, Y. Liu, and T. Wang, "Increasing signalized intersection capacity with unconventional use of special width approach lanes," *Comput.-Aided Civil Infrastruct. Eng.*, vol. 31, no. 10, pp. 794–810, Jun. 2016.

[18] J. Zhao, W. Ma, H. M. Zhang, and X. Yang, "Increasing the capacity of signalized intersections with dynamic use of exit lanes for left-turn traffic," *Transp. Res. Rec.*, vol. 2355, no. 1, pp. 49–59, Jan. 2013.

[19] J. Wu, P. Liu, Z. Z. Tian, and C. Xu, "Operational analysis of the contraflow left-turn lane design at signalized intersections in china," *Transp. Res. C, Emerg. Technol.*, vol. 69, pp. 228–241, Aug. 2016.

[20] B. Heydecker, "Uncertainty and variability in traffic signal calculations," *Transp. Res. B, Methodol.*, vol. 21, no. 1, pp. 79–85, Feb. 1987.

[21] S. H. Hamdar, H. S. Mahmassani, and M. Treiber, "From behavioral psychology to acceleration modeling: Calibration, validation, and exploration of drivers' cognitive and safety parameters in a risk-taking environment," *Transp. Res. B, Methodol.*, vol. 78, pp. 32–53, Aug. 2015.

[22] X. Jiang and H. Adeli, "Wavelet packet-autocorrelation function method for traffic flow pattern analysis," *Comput.-Aided Civil Infrastruct. Eng.*, vol. 19, no. 5, pp. 324–337, Sep. 2004.

[23] Y. Yin, "Robust optimal traffic signal timing," *Transp. Res. B, Methodol.*, vol. 42, no. 10, pp. 911–924, Dec. 2008.

[24] J. Zhao, J. Yu, and X. Zhou, "Saturation flow models of exit lanes for left-turn intersections," *J. Transp. Eng. A, Syst.*, vol. 145, no. 3, Mar. 2019, Art. no. 04018090.

[25] P. Su, C. Krause, D. Hale, J. Bared, and Z. Huang, "Operational advantages of contraflow left-turn pockets at signalized intersections," *Inst. Transp. Eng.*, vol. 86, p. 44, Jul. 2016.

[26] P. Liu, J. Wu, H. Zhou, J. Bao, and Z. Yang, "Estimating queue length for contraflow left-turn lane design at signalized intersections," *J. Transp. Eng. A, Syst.*, vol. 145, no. 6, Jun. 2019, Art. no. 04019020.

[27] J. Wu, P. Liu, X. Qin, H. Zhou, and Z. Yang, "Developing an actuated signal control strategy to improve the operations of contraflow left-turn lane design at signalized intersections," *Transp. Res. C, Emerg. Technol.*, vol. 104, pp. 53–65, Jul. 2019.

[28] J. Zhao, M. Yun, H. M. Zhang, and X. Yang, "Driving simulator evaluation of drivers' response to intersections with dynamic use of exit-lanes for left-turn," *Accident Anal. Prevention*, vol. 81, pp. 107–119, Aug. 2015.

[29] J. Zhao and Y. Liu, "Safety evaluation of intersections with dynamic use of exit-lanes for left-turn using field data," *Accident Anal. Prevention*, vol. 102, pp. 31–40, May 2017.

[30] S. Yang, B. Yang, H.-S. Wong, and Z. Kang, "Cooperative traffic signal control using multi-step return and off-policy asynchronous advantage actor-critic graph algorithm," *Knowl.-Based Syst.*, vol. 183, Nov. 2019, Art. no. 104855.

[31] Y. Zhang and Y. Zhou, "Distributed coordination control of traffic network flow using adaptive genetic algorithm based on cloud computing," *J. Netw. Comput. Appl.*, vol. 119, pp. 110–120, Oct. 2018.

[32] S.-W. Chiou, "A data-driven bi-level program for knowledge-based signal control system under uncertainty," *Knowl.-Based Syst.*, vol. 160, pp. 210–227, Nov. 2018.

[33] J. Zhao and X. Zhou, "Improving the operational efficiency of buses with dynamic use of exclusive bus lane at isolated intersections," *IEEE Trans. Intell. Transp. Syst.*, vol. 20, no. 2, pp. 642–653, Feb. 2019.

[34] P. C. M. Ribeiro, "Handling traffic fluctuation with fixed-time plans calculated by TRANSYT," *Traffic Eng. Control*, vol. 35, pp. 362–366, Jun. 1994.

[35] B. Park and A. Kamarajugadda, "Development and evaluation of a stochastic traffic signal optimization method," *Int. J. Sustain. Transp.*, vol. 1, no. 3, pp. 193–207, Jul. 2007.

[36] J.-Q. Li, "Discretization modeling, integer programming formulations and dynamic programming algorithms for robust traffic signal timing," *Transp. Res. C, Emerg. Technol.*, vol. 19, no. 4, pp. 708–719, Aug. 2011.

[37] Y. Tong, L. Zhao, L. Li, and Y. Zhang, "Stochastic programming model for oversaturated intersection signal timing," *Transp. Res. C, Emerg. Technol.*, vol. 58, pp. 474–486, Sep. 2015.

[38] C. Yu, W. Ma, H. K. Lo, and X. Yang, "Robust optimal lane allocation for isolated intersections," *Comput.-Aided Civil Infrastruct. Eng.*, vol. 32, no. 1, pp. 72–86, Nov. 2016.

[39] W. Hao, C. Ma, B. Moghimi, Y. Fan, and Z. Gao, "Robust optimization of signal control parameters for unsaturated intersection based on tabu search-artificial bee colony algorithm," *IEEE Access*, vol. 6, pp. 32015–32022, 2018.

[40] L. Zhang, Y. Yin, and Y. Lou, "Robust signal timing for arterials under Day-to-Day demand variations," *Transp. Res. Rec.*, vol. 2192, no. 1, pp. 156–166, Jan. 2010.

[41] K. Wada, K. Usui, T. Takigawa, and M. Kuwahara, "An optimization modeling of coordinated traffic signal control based on the variational theory and its stochastic extension," *Transp. Res. Procedia*, vol. 23, pp. 624–644, Jan. 2017.
[42] H. He, S. I. Guler, and M. Menendez, "Adaptive control algorithm to provide bus priority with a pre-signal," *Transp. Res. C, Emerg. Technol.*, vol. 64, pp. 28–44, Mar. 2016.
[43] O. J. Ibarra-Rojas, F. Delgado, R. Giesen, and J. C. Muñoz, "Planning, operation, and control of bus transport systems: A literature review," *Transp. Res. B, Methodol.*, vol. 77, pp. 38–75, Jul. 2015.
[44] W. Gu, M. J. Cassidy, V. V. Gayah, and Y. Ouyang, "Mitigating negative impacts of near-side bus stops on cars," *Transp. Res. B, Methodol.*, vol. 47, pp. 42–56, Jan. 2013.
[45] R. X. Zhong, C. Chen, Y. P. Huang, A. Sumalee, W. H. K. Lam, and D. B. Xu, "Robust perimeter control for two urban regions with macroscopic fundamental diagrams: A control-Lyapunov function approach," *Transp. Res. Procedia*, vol. 23, pp. 922–941, Jan. 2017.
[46] K. Ampountolas, N. Zheng, and N. Geroliminis, "Macroscopic modelling and robust control of bi-modal multi-region urban road networks," *Transp. Res. B, Methodol.*, vol. 104, pp. 616–637, Oct. 2017.
[47] S. P. Hoogendoorn, V. L. Knoop, and H. J. van Zuylen, "Robust control of traffic networks under uncertain conditions," *J. Adv. Transp.*, vol. 42, no. 3, pp. 357–377, Jul. 2008.
[48] W. Szeto and H. K. Lo, "Strategies for road network design over time: Robustness under uncertainty," *Transportmetrica*, vol. 1, pp. 47–63, Jan. 2005.
[49] K. Han, H. Liu, V. V. Gayah, T. L. Friesz, and T. Yao, "A robust optimization approach for dynamic traffic signal control with emission considerations," *Transp. Res. C, Emerg. Technol.*, vol. 70, pp. 3–26, Sep. 2016.
[50] X. Li and J.-Q. Sun, "Signal multiobjective optimization for urban traffic network," *IEEE Trans. Intell. Transp. Syst.*, vol. 19, no. 11, pp. 3529–3537, Nov. 2018.
[51] X. Li and J.-Q. Sun, "Turning-lane and signal optimization at intersections with multiple objectives," *Eng. Optim.*, vol. 51, no. 3, pp. 484–502, Jul. 2018.
[52] J. M. Mulvey, R. J. Vanderbei, and S. A. Zenios, "Robust optimization of large-scale systems," *Oper. Res.*, vol. 43, no. 2, pp. 264–281, Apr. 1995.
[53] *Highway Capacity Manual 2010*, Transp. Res. Board, Washington, DC, USA, 2010.
[54] C. K. Wong and S. C. Wong, "Lane-based optimization of signal timings for isolated junctions," *Transp. Res. B, Methodol.*, vol. 37, no. 1, pp. 63–84, Jan. 2003.
[55] C. K. Wong and S. C. Wong, "A lane-based optimization method for minimizing delay at isolated signal-controlled junctions," *J. Math. Model. Algorithms*, vol. 2, no. 4, pp. 379–406, 2003.
[56] Z. Li, "Modeling arterial signal optimization with enhanced cell transmission formulations," *J. Transp. Eng.*, vol. 137, no. 7, pp. 445–454, Jul. 2011.
[57] L. Zhang, Y. Yin, and S. Chen, "Robust signal timing optimization with environmental concerns," *Transp. Res. C, Emerg. Technol.*, vol. 29, pp. 55–71, Apr. 2013.
[58] C. K. Wong and B. G. Heydecker, "Optimal allocation of turns to lanes at an isolated signal-controlled junction," *Transp. Res. B, Methodol.*, vol. 45, no. 4, pp. 667–681, May 2011.

KAIJIA CHEN was born in Haimen, Jiangsu, China, in 1995. He received the B.S. degree in traffic engineering from Nantong University, Jiangsu, in 2017. He is currently pursuing the master's degree with the Traffic Engineering Department, University of Shanghai for Science and Technology.

His research interests include signal control and optimization algorithm.

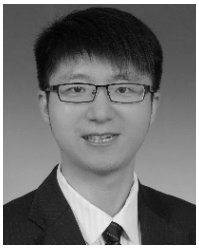

JING ZHAO was born in Shanghai, China, in 1983. He received the B.S., M.S., and Ph.D. degrees in traffic engineering from Tongji University, Shanghai, China, in 2002, 2009, and 2014, respectively.

From 2014 to 2016, he was an Assistant Professor with the Traffic Engineering Department, University of Shanghai for Science and Technology, Shanghai, China, where he has been an Associate Professor, since 2017. He is the first author of more than 30 articles in peer-reviewed journals. His research interests include signal control, traffic design, and bus transit systems.

VICTOR L. KNOOP was born in The Netherlands, in 1981. He received the M.S. degree in physics from Leiden University, in 2005, and the Ph.D. degree from the Delft University of Technology, in 2009, on the effects of incidents on driving behavior and traffic congestion.

He held a postdoctoral position at the University of Lyon, from 2009 to 2010, on lane changing. He held a Tenured Assistant Professorship at the Delft University of Technology, from 2010 to 2017, where he has been a Tenured Associate Professor with the Transport and Planning Department, since 2018. His main research interest is the interaction between microscopic and macroscopic traffic flow phenomena.

XING GAO was born in Anda, Heilongjiang, China, in 1997. She received the B.S. degree in traffic engineering from Shanghai Maritime University, Shanghai, China, in 2018. She is currently pursuing the master's degree with the Traffic Engineering Department, University of Shanghai for Science and Technology.

Her research interests include traffic design and signal control.